

MulticARRIER Trapping by Copper Microprecipitates in Silicon

A. Broniatowski

Groupe de Physique des Solides, Université de Paris VII, 2, Place Jussieu, 75251 Paris CEDEX 05, France

(Received 6 January 1989)

In a simple model based on the Schottky-Mott theory of metal-semiconductor contacts, a metallic precipitate in a semiconducting matrix has the properties of a multicARRIER, amphoteric trap. A use is made of this model to analyze the trapping effects of copper-decorated twinned boundaries in silicon bicrystals. The model gives, in particular, a simple explanation for the emission properties of the boundary traps, as determined by deep-level-transient-spectroscopy experiments on the bicrystals.

PACS numbers: 71.55.Ht, 61.70.Ng, 73.40.Vz

Metal impurities, when diffused in a semiconductor, are usually found to segregate on lattice defects such as dislocations, grain boundaries, and heterointerfaces.¹ Drastic changes will then result in the electronic properties of the material.^{2,3} Our purpose in this connection is to investigate the effects of a copper precipitation on twinned boundaries in silicon bicrystals. Twinned boundaries are generally not expected to contain carrier traps because of the coincident lattice matching. When decorated with copper microprecipitates, however, the same boundaries exhibit strong barrier effects and a large recombination efficiency. Attention is thus drawn on the trapping effects of the precipitates. In a simple model based on the Schottky-Mott theory of metal-semiconductor contacts, to be discussed below, a metallic

precipitate in a semiconducting matrix has the properties of a multicARRIER, amphoteric trap. We shall make use of this model to analyze the role of the precipitates in the electrical activity of the boundaries. The model provides, in particular, a simple explanation for the emission properties of the grain boundary traps, as determined by deep-level-transient-spectroscopy (DLTS) experiments on the bicrystals.

The material for these investigations are *n*-type (phosphorus doped to $3.6 \times 10^{14} \text{ cm}^{-3}$) and *p*-type (boron doped to $8.0 \times 10^{14} \text{ cm}^{-3}$) bicrystals with the $\Sigma=25$ boundary (twin plane $\{710\}$, tilt axis $\langle 001 \rangle$, tilt angle 16.26°).⁴ The boundary in as-grown specimens has no detectable electrical effects. Samples of both types have been contaminated with copper and then subjected to annealing treatments for several hours at 900°C , resulting in the precipitation of a copper silicide phase on the boundary.⁵ A fraction of the precipitates are gathered in colonies (Fig. 1). The precipitates have a polyhedral shape with typical sizes of a few tens of nm. The density of precipitates is estimated on the order of $10^{10}/\text{cm}^2$ in the boundary plane.

Decoration with copper makes the boundary electrical active, as barrier effects are now obtained in both types of bicrystals. The properties of the grain boundary states have been investigated by DLTS⁶ in the modalities of Ref. 7. Briefly summarized, the experiment consists of applying periodic voltage pulses across the boundary in order to vary the occupancy of the traps. The emission transients are detected by the concomitant variation of the boundary capacitance. The DLTS signal is formed by processing the transients through a dual-gate correlator. By recording the signal as a function of the sample temperature, a spectrum characteristic of the boundary states is obtained. Figure 2 represents in the solid lines a set of boundary spectra for a *p*-type bicrystal: In 2(a) for different pulse amplitudes and in 2(b) for different gate settings. Salient features of the spectra are as follows: (i) All the spectra are in the form of a peak, indicative of a single, or a narrowly distributed group of energy levels. (ii) The peak amplitude has no apparent saturation for voltage pulses up to 80 V. (iii)

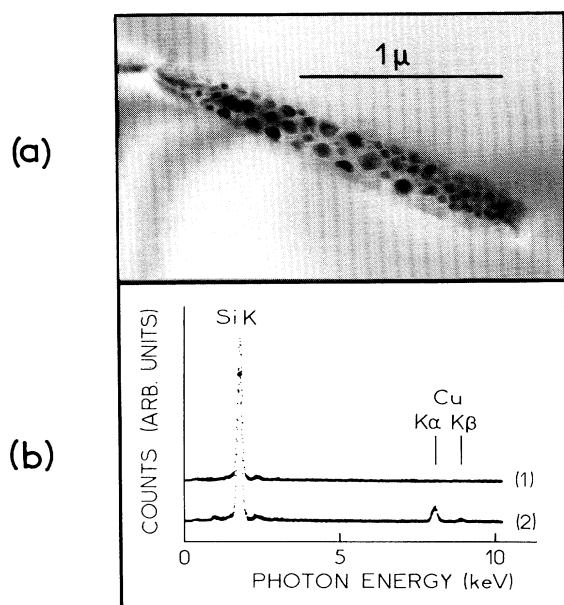


FIG. 1. (a) Bright-field transmission-electron micrograph of a colony of copper-rich precipitates in the boundary plane. (b) Energy-dispersive x-ray analysis of the silicon matrix [spectrum (1)], and the copper precipitates [spectrum (2)].

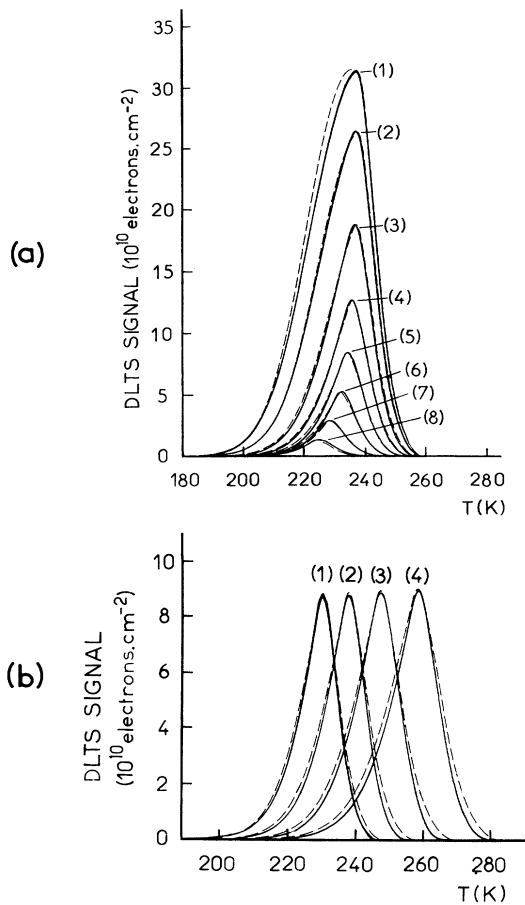


FIG. 2. (a) DLTS spectra of the grain boundary states in a *p*-type bicrystal for different pulse amplitudes: (1) 80 V; (2) 45 V; (3) 16 V; (4) 8 V; (5) 3.5 V; (6) 1.7 V; (7) 0.75 V; (8) 0.30 V; gate settings $t_1=35$ ms, $t_2=135$ ms; bias voltage 0 V; pulse duration 40 ms. The solid lines are experimental recordings and the dotted lines are computer simulations using Eq. (2). (b) Same as (a), for different gate settings: (1) $t_1=85$ ms, $t_2=340$ ms; (2) $t_1=25$ ms, $t_2=100$ ms; (3) $t_1=7$ ms, $t_2=28$ ms; (4) $t_1=1.75$ ms, $t_2=7.00$ ms; pulse amplitude 4 V; bias voltage 0 V.

The temperature of the maximum in the spectra has a gradual shift as the pulse amplitude increases. Spectra with similar features are also obtained in the *n*-type bicrystals following a copper precipitation on the boundary.

Our hypothesis to explain these spectra is that the boundary traps originate from the precipitates in the boundary plane [Fig. 3(a)]. Silicon and copper give a number of electron (or Hume Rothery) phases with a metallic character.⁸ Let us then assume that the precipitates, being metallic in nature, form a rectifying contact with the silicon matrix. A precipitate thus constitutes a potential well for the carriers. According to the Schottky-Mott theory of metal-semiconductor con-

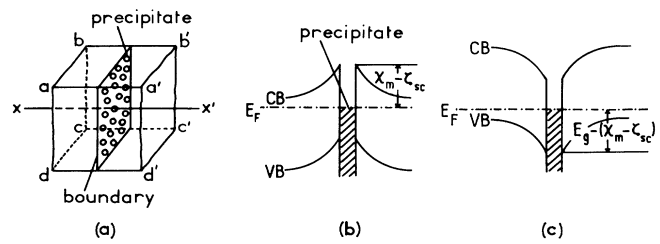


FIG. 3. (a) Schematic representation of the copper precipitates in the boundary plane, showing in *abcd* and *a'b'c'd'* the left and the right edges of the space-charge region, respectively; *xx'* is a line through a precipitate in the direction normal to the boundary. (b), (c) Bendings of the energy bands along *xx'* in an *n*- and in a *p*-type specimen, respectively. VB, valence band and CB, conduction band of the semiconductor; E_F , Fermi level; χ_m , work function of the precipitate; ζ_{sc} and E_g , electron affinity and band gap of the semiconductor, respectively.

tacts,^{9,10} the Fermi energy of the precipitate is located at a distance $\chi_m - \zeta_{sc}$ below the conduction-band edge at the semiconductor-precipitate interface [Fig. 3(b)], where χ_m is the work function of the precipitate, and ζ_{sc} is the electron affinity of the semiconductor. The energy E_a to promote an electron into the conduction band (respectively, a hole into the valence band) is thus $\chi_m - \zeta_{sc}$ [respectively, $E_g - (\chi_m - \zeta_{sc})$], where E_g is the band gap of the semiconductor. In this model, a precipitate has therefore the properties of a deep acceptor in *n*-type [Fig. 3(b)], and of a deep donor in *p*-type material [Fig. 3(c)], respectively. The boundary charge in equilibrium is about 10^{11} carriers/cm², corresponding to a net charge of some ten carriers per precipitate. In view of the small spacing of the precipitates, the space-charge regions around them broadly overlap, resulting in a continuous (though not homogeneous) potential barrier alongside the boundary plane.

As voltage pulses are applied through the boundary, additional carriers become trapped on the precipitates [Fig. 4(a)]. The boundary then relaxes towards equilibrium by thermal emission of the excess carriers [Fig. 4(b)]. It is understood in the present model that a pre-

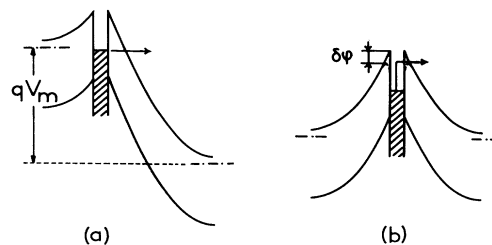


FIG. 4. (a) Bending of the energy bands under voltage V_m ; the arrow represents the field-emission process. (b) Relaxation of the excess charge on a precipitate by thermionic emission (arrow); $\delta\phi$ is the image-force lowering of the work function due to the electric field at the matrix-precipitate interface.

precipitate has a metal-like density of states, and that its emissive properties therefore follow the thermionic emission law. To obtain the form of the emission transients, let us assimilate the precipitates to spherical particles of radius a , and density N in the boundary plane. The current flow from a precipitate is given by $4\pi a^2 A^* T^2 \exp(-E_a/k_B T) \exp(\delta\phi/k_B T)$, where $4\pi a^2$ represents the emissive area of the precipitate, A^* is an effective Richardson constant, and $\delta\phi$ is the image-force lowering of the work function due to the electric field E at the matrix-precipitate interface. The variation rate of the boundary charge is then obtained by adding up the contributions of the various precipitates, as follows:

$$d|Q|/dt = -\Phi A^* T^2 \exp(-E_a/k_B T) \times \exp(\delta\phi/k_B T), \quad (1)$$

where $\Phi = 4\pi a^2 N$ is the emissive surface of the precipitates per unit boundary area. The limitation of Eq. (1) is that it does not take capture into account. Carrier trapping will actually become important only in the final part of the transient, where the barrier height does not exceed that of equilibrium by more than a few $k_B T$. To obtain $\delta\phi$, we note that the field on the surface of a precipitate is predominantly that of its own charge: $E \approx Q/4\pi\epsilon a^2 N$, where ϵ is the dielectric constant of the semiconductor. $\delta\phi$ is then given approximately by¹¹ $(q/2\epsilon)(q|Q|/\pi\Phi)^{1/2}$, where q is the elementary positive charge. Taking Q as the independent variable, Eq. (1) integrates explicitly to give the following:

$$t + t_0 = 8\pi(\epsilon k_B)^2 (q^3 A^*)^{-1} (u + 1) \times \exp(-u) \exp(E_a/k_B T) \quad (2)$$

with the auxiliary variable $u = (q/2\epsilon k_B T)(q|Q|/\pi\Phi)^{1/2}$. (In this calculation, E_a is taken to be constant with respect to the charge on the precipitates. Typical variations of the charge in these experiments amount to a few tens of carriers per precipitate only. Such variations will only cause minute changes in the Fermi energy of the precipitates.) The integration constant t_0 relates to the magnitude of the boundary charge Q_m for $t=0$, the beginning of the emission transient. Q_m depends in turn on the amplitude of the filling pulses, and is determined experimentally by the means of low-temperature capacitance-voltage measurements.⁷ Figure 2 represents in the dotted lines computer simulations of the spectra using Eq. (2) for the emission transients. The best fit one obtains is with $E_a = 0.69 \pm 0.02$ eV, $\Phi = 0.12 \pm 0.02$, and $A^* = (7 \pm 1) \times 10^5$ $\text{A m}^{-2} \text{K}^{-2}$. With this set of values, the simulations reproduce the recorded spectra accurately, particularly the temperature shifts of the maximum in relation to the filling pulse amplitude [Fig. 2(a)] and the gate settings [Fig. 2(b)]. A similar fit is obtained for the spectra of the n -type bicrystal, with $E_a = 0.55 \pm 0.02$ eV, $\Phi = 0.10 \pm 0.02$, and $A^* = (1.4 \pm 0.2) \times 10^6$ $\text{A m}^{-2} \text{K}^{-2}$. The values of A^* in both

types of samples are of the order of the theoretical Richardson constant, 1.2×10^6 $\text{A m}^{-2} \text{K}^{-2}$. These data altogether confirm the validity of the model to describe the trapping effects of the precipitates in both types of specimens.

It is of interest to consider the significance of the temperature shift of the spectra in Fig. 2(a) in relation to the thermionic emission law. Let us neglect the image-force lowering of the barrier, which amounts to taking $\delta\phi=0$ in Eq. (1): To this approximation, the boundary charge relaxes to equilibrium with the constant rate $-\Phi A^* T^2 \exp(-E_a/k_B T)$, so that the emission transient assumes the shape of a straight line. It is easily seen that the spectra associated with such transients have a shift of their maximum to higher temperatures for increasing values of the boundary charge. The shift is actually compensated in part by the lowering of the barrier to emission, leading to the observed dependence of the spectra on the pulse amplitude in Fig. 2. A similar shift to higher temperatures is to be expected more generally in cases where the release of the trapped carriers obeys the thermionic emission law. A prior work by Martin *et al.*¹² suggests, in particular, that the same effect may appear in DLTS studies of quantum-well heterostructures.

It follows from this analysis of the spectra, that a precipitate has the properties of a multicarrier trap. The question then arises of the maximum charge on a precipitate. The charging of the precipitates will be limited ultimately by the onset of field emission [Fig. 4(a)]. The critical field for this process is given approximately by¹³ $E_{FE} = (2m^* E_a^3)^{1/2} / \hbar q$, where m^* represents an effective mass of the carriers in the semiconductor. With the typical value $E_a = 0.5$ eV, E_{FE} is about 10^7 V/cm. A precipitate of a few tens of nm in size will then have a limiting charge of the order of 10^4 carriers. As mentioned before, the typical charges of the precipitates in the DLTS experiments are only a small fraction of this limiting value.

In the band scheme of Fig. 3, the trap level E_a is determined by the contact properties between the phase precipitated and the semiconducting matrix. For a more detailed analysis, however, size effects should also be taken into account. The Fermi energy of a metallic precipitate depends upon its size, due to the quantum-mechanical effect of confining the electrons. A simple estimate¹⁴ for the shift of the Fermi energy in a precipitate of size a gives $\delta E_F \approx (\hbar\pi a)(E_F/m^{**})^{1/2}$, where m^{**} is an effectively mass of the electrons and E_F is the Fermi energy of the metallic phase. Taking for E_F the value of 5 eV typical of a metal and for m^{**} the free electron mass, one finds for $a = 20$ nm, $\delta E_F \approx 0.02$ eV. The work function of the precipitate (hence the energy E_a) will also be changed by this amount. One thus expects a dispersion in the energies of the traps, the more pronounced as the precipitates are small. Variations have been effectively noted in the shape of the grain boundary

spectra, depending on the rate of copper precipitation.⁵ These effects are currently being investigated.

The emphasis in this study has been laid on the emission, rather than the capture properties, of the precipitates. By analogy with the case of hot electron devices¹⁵ one should expect inelastic collisions with the conduction electrons of the precipitates to play an important role in the capture processes. More information will be needed on the electron properties of the phase precipitated, however, before definite conclusions can be drawn in this matter.

There has been a long-standing discussion on the role of segregated impurities in making the boundaries electrically active.¹⁶ Oxygen in silicon has thus been frequently advocated.¹⁷ This study has emphasized, on the other hand, the effects of a copper precipitation. One should expect, in the more general case, a combined effect of the different segregated species, depending on the impurity content and the thermal history of the material. There is, therefore, a need for a better understanding of the chemistry and the kinetics of impurity segregation on the boundaries, particularly in the case of the fast-diffusing transition metals in silicon.

I am indebted to M. Astier, A. Mauger, and J. Zizine for numerous stimulating discussions, and especially to C. Colliex and J. L. Maurice for permission to reproduce their electron microscopy observations.

¹W. C. Dash, *J. Appl. Phys.* **27**, 1193 (1956).

²A. Goetzberger and W. Shockley, *J. Appl. Phys.* **31**, 1821 (1960).

³W. Shockley, *Solid-State Electron.* **2**, 35 (1961).

⁴The bicrystals have been grown by Cristaltec (Centre d'Etudes Nucléaires de Grenoble, France).

⁵M. Aucouturier, A. Broniatowski, A. Chari, and J. L. Maurice, in "Polycrystalline Semiconductors," edited by J. Werner (Springer-Verlag, Berlin, to be published).

⁶D. V. Lang, *J. Appl. Phys.* **45**, 3023 (1974).

⁷A. Broniatowski, *Phys. Rev. B* **36**, 5895 (1987).

⁸N. F. Mott and H. Jones, *The Theory of the Properties of Metals and Alloys* (Dover, New York, 1958), p. 169ff.

⁹N. F. Mott, *Proc. Roy. Soc. London A* **171**, 27 (1939).

¹⁰W. Schottky, *Z. Phys.* **113**, 367 (1939).

¹¹See, e.g., E. H. Rhoderick, *Metal-Semiconductor Contacts* (Clarendon, Oxford, 1978), p. 39; B. R. Gossick, *Potential Barriers in Semiconductors* (Academic, New York, 1964), Chap. 2.

¹²P. A. Martin, K. Meehan, P. Gavrilovic, K. Hess, N. Holonyak, and J. J. Coleman, *J. Appl. Phys.* **54**, 4689 (1983).

¹³Rhoderick, Ref. 11, p. 98.

¹⁴C. Herring and M. H. Nichols, *Rev. Mod. Phys.* **21**, 185 (1949).

¹⁵S. M. Sze, *Physics of Semiconductor Devices* (Wiley, New York, 1969), Chap. 11, and references therein.

¹⁶For a review, see C. R. M. Grovenor, *J. Phys. C* **18**, 4079 (1985).

¹⁷L. L. Kazmerski, *J. Vac. Sci. Technol.* **20**, 423 (1982).

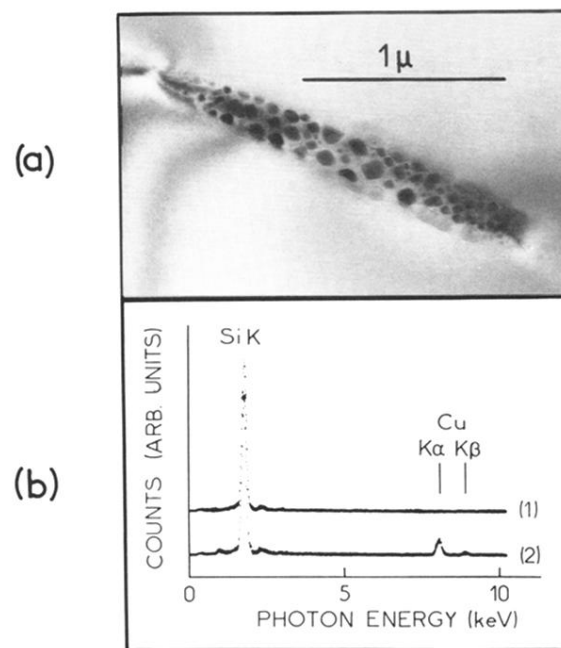


FIG. 1. (a) Bright-field transmission-electron micrograph of a colony of copper-rich precipitates in the boundary plane. (b) Energy-dispersive x-ray analysis of the silicon matrix [spectrum (1)], and the copper precipitates [spectrum (2)].